Effect of Indium Doping Zinc Sulfide Nanostructures on the Physical and Sensing Properties via Chemical Spray Pyrolysis

Tahseen H. Mubarak[1], Oday Ali Chichan[2], Jenan Abdullah Khlati[3], Shaymaa A. Hussein[4], Hanaa Kadem Essa[3], Nadir Fadhil Habubi[3,5,6], Sami Salman Chiad[3] and Yassin Hasan Kadhim[7]

[1]*Department of Physics, College of Science, University of Diyala, 32001 Baqubah, Diyala, Iraq*
[2]*Department of Physics, College of Education for Pure Sciences, University of Babylon, 51001 Hillah, Babil, Iraq*
[3]*Department of Physics, College of Education, Mustansiriyah University, 10052 Baghdad, Iraq*
[4]*Department of Medical Laboratory Techniques, Al-Manara College for Medical Science, 62001 Al-Amarah, Maysan Governorate, Iraq*
[5]*Department of Radiation and Sonar Technologies, Alnukhba University College, 10013 Baghdad, Iraq*
[6]*Department of Radiology Techniques, Al-Qalam University College, 36001 Kirkuk, Iraq*
[7]*Department of Optics Techniques, College of Health and Medical Techniques, AL-Mustaqbal University, 51001 Hillah, Babylon, Iraq*
dean@sciences.uodiyala.edu.iq, dr.sami@uomustansiriyah.edu.iq, nadirfadhil@uomustansiriyah.edu.iq, yassin.hasan@uomus.edu.iq, shaimaa2021@uomanara.edu.iq, jenanabdullah@uomustansiriyah.edu.iq, hanaa.kadhem@uomustansiriyah.edu.iq, pure.oday.ali@uobabylon.edu.iq

Keywords: ZnS, Spray Pyrolysis, Optical, XRD, AFM, Band Gap Energy, Resistance and Sensitivity.

Abstract: Indium-doped ZnS samples with doping levels of 0%, 1%, and 3% were fabricated using the chemical spray pyrolysis (CSP) method. XRD patterns confirmed the presence of a cubic zinc blend structure of both pure and Indium-doped ZnS samples. The crystallite size slightly increased with the concentration of indium, attributed to the substitution of indium within the ZnS lattice. AFM provided microscopic insights into the surface structure, allowing for the visualization and characterization of surface topographies. SEM images show transformation in ZnS films with Indium doping: flat islands to spherical nano-grains, indicating size reduction correlating with Indium concentration, influenced by ZnS-Indium interaction during synthesis. The optical parameters of nanostructures were investigated with doping and the incorporation of indium substitute for Zn ions. Indium doping in ZnS films increases resistance and alters gas sensing properties by affecting charge carrier mobility and adsorption efficiency. Higher Indium doping in ZnS films reduces sensitivity to NO_2 gas due to changes in charge carrier mobility and film structure.

1 INTRODUCTION

ZnS is a material that occurs naturally, that is plentiful, non-toxic, safe for the environment, and chemically unchanging [1]. It exists in two crystalline forms: cubic zinc-blend at low and wurtzite at high temperatures [2], [3]. Both forms of ZnS have a large bandgap, approximately 3.54-3.91 eV, respectively [4], [5]. Additionally, ZnS exhibits high transmittance, a large dielectric constant, and a high refractive index [6]-[9]. Elements such as Al, In, Cr, Ga, F, Cu, Cl, B, and Mn, at different doping content to alter ZnS's characteristics [10]-[13]. It is widely recognized that the ionic radius of In^{3+} (0.80 Å) closely matches that of Zn^{2+} (0.74 Å), making it plausible to assume that the incorporation of indium into the ZnS lattice or its substitution for Zn^{2+} is feasible [14]. Various chemical techniques have been employed for this purpose, including electrodeposition [15], chemical bath deposition [16], [17], sol-gel, spin coating [18], and spray pyrolysis [19], [20]. CSP is characterized by its simplicity, cost-effectiveness, and adaptability to large-scale processing. This research attempts to look into the effects of In^{3+} ion doping on the synthesis, structural characteristics, surface topography, and optical properties of ZnS nanofilms.nano films.

2 EXPERIMENTAL

A high-purity 0.1 M solution of $ZnCl_4 \cdot 5H_2O$ was used as the zinc source, dissolved in 100 ml of redistilled water to form the precursor solution. The preparation

conditions were optimized to achieve highly homogeneous thin films. A 0.1 M solution of Indium trichloride ($InCl_3$) was used as the dopant and added to the base solution to achieve doping levels of 1% and 3%. The solution was sprayed onto clean, preheated glass substrates at a temperature of 400 °C, nozzle-to-substrate distance of 28 cm. Spraying was performed for 9 seconds with 50-second intervals to prevent substrate cooling. The spray rate was maintained at 5 ml/min, and nitrogen gas was used as a carrier.

Film thickness was measured by gravimetric method discovered to be nearly 320 ± 20 nm. X-ray diffraction analysis was performed using a Shimadzu 6-2000 instrument with CuKα radiation, where the wavelength (λ) was 0.15406 nm. Surface morphology was investigated using electron surface microscopy (Hitachi S-4160). Additionally, Optical measurements were done by a Cary 100 UV-Visible spectrophotometer. Gas sensitivity is typically assessed by cylindrical chamber with a radius of 8 cm and a height of 14 cm.

3 RESULTS AND DISCUSSIONS

3.1 X-Ray Analysis

XRD patterns of intended films are offered in Figure 1. Patterns show that every sample has the cubic zinc blend structure, which closely matches ICDD card No. 5-0566. The greatest noticeable peak is in line with the lattice plane (111), while additional peaks corresponding to lattice planes (220), (311), and (400) are observed with varying intensities. The diffraction pattern of In^{3+} doped ZnS exhibits apparent shifts towards higher 2θ as the concentration of In^{3+} rises. This increase in the diffraction angle results from lattice contraction expected due to the higher surface-to-volume ratio [21]. The average grain size (*D*) was calculated by Scherrer formula [22]:

$$D = \frac{K\lambda}{\beta cos\theta}. \quad (1)$$

where *k* is 0.94, λ is the wavelength of X-rays, θ is Bragg angle Hence, by using the above relation, D of ZnS nanostructures doped with different concentrations of In^{3+} lies between 15.18 nm and 17.82 nm for pure ZnS and doping. A dislocation represents a structural defect within a crystal caused by a mismatch in lattice alignment between different crystal regions. In other words, their presence and density cannot be solely explained by thermodynamic considerations. The dislocation density (δ) was established by (2) [23]:

$$\delta = \frac{1}{D^2}. \quad (2)$$

The strain was established using the following relation [24]:

$$\varepsilon = \frac{\beta cos\theta}{4}. \quad (3)$$

Figure 2 outlines *D*, ε, and δ of ZnS nanostructures doped with different contents of In^{3+}. Table reveals that ε and δ decrease as the *D* increases. The decreased values of δ and ε observed with Indium doping indicate a reduction in crystal defects as can be seen in Figure 2. This effect is attributed to acting as an enhancer rather than an inhibitor [25].

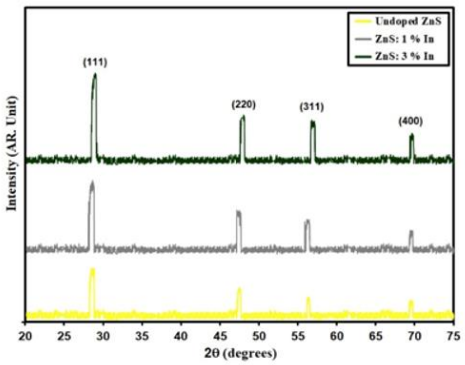

Figure 1: XRD styles of grown films.

3.2 Surface Topography Analysis

Figure 3 offers AFM images of the intended films. The average particle size of Pav decreases (from 78.1 nm to 31.5 nm) with increment doping of In3+ from a 3% concentration. The films exhibit uniform, well-defined, spherical morphology. pav reduces with Indium content., which agrees with [26]. In It is evident that at higher doping levels, the growth of thin films exhibited lower roughness (Ra). The root mean square (RMS) roughness was reported in Table 1. The reduction in particle size can be correlated with substituting In3+ ions, yielding similar results as reported elsewhere [27], [28].

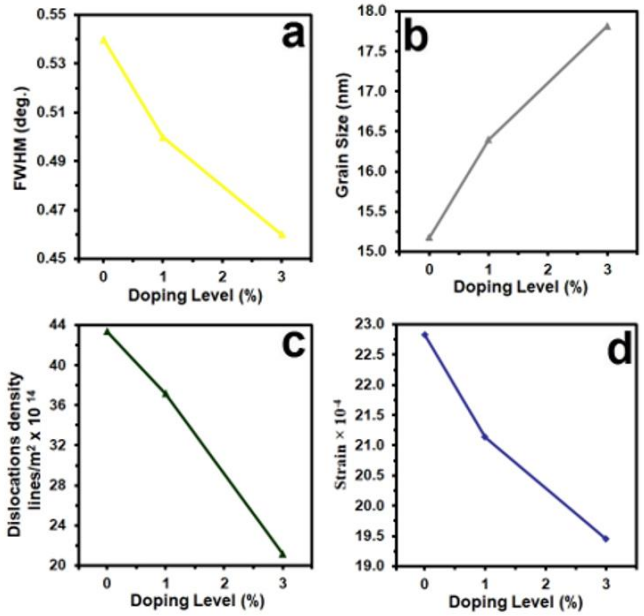

Figure 2: FWHM, strain and dislocation of pure and ZnS: In films with different dopant.

Table 1: AFM parameters of the intended films.

Samples	Average Particle size nm	R_a (nm)	R. M. S. (nm)
Undoped ZnS	78.1	9.29	8.73
ZnS: 1% In	75.8	4.15	5.91
ZnS: 3% In	31.5	3.66	3.31

3.3 Optical Analysis

Experimental measurements are often presented in terms of percentage transmittance (T), as defined in (4) [38]-[40]:

$$T\% = \frac{I}{I_o}\% \,. \tag{4}$$

Where I_o and I represent the initial and measured light intensities, respectively. T spectra are illustrated in Figure 4. Films exhibit high intensity across the visible light area, with lower transmission intensity observed at higher Indium concentrations. To some extent, this phenomenon could be attributed to surface roughening at higher dopant ratios [41], [42]. Notably, higher intensity was observed in the higher wavelength region of the visible light spectrum. These data assure active role of indium as a dopant in broadening the absorption spectrum of the resulting film [43], [44].

The absorption coefficient (α) was calculated via the following (5) [45]:

$$\alpha = \frac{(lnT^{-1})}{t} \,. \tag{5}$$

Where t is film thickness. From Figure 5, it is evident that the absorption coefficient value exceeds 10^4 cm^{-1}, which indicates a transition between the extended states in the valence band (VB) and the conduction band (CB). Additionally, a noticeable shift of the absorption edge towards lower energies is observed with increasing indium concentration [46], [47]. This shift signifies a decrease in E_g with increasing Indium content, as illustrated in Figure 5. Similar observations have been reported in previous studies [48].

The gap energy (E_g) of our films was determined using Tauc relation [50]:

$$\alpha hv = B(hv - E_g)^r. \tag{6}$$

Where B is a constant, and the exponent r takes values of 1/2 for direct. The resulting plots are depicted in Figure 6, which show that the deposited films are determined to be 3.59 eV, 3.55 eV, and 3.50 eV, respectively. These results agree with Geng et al. [51].

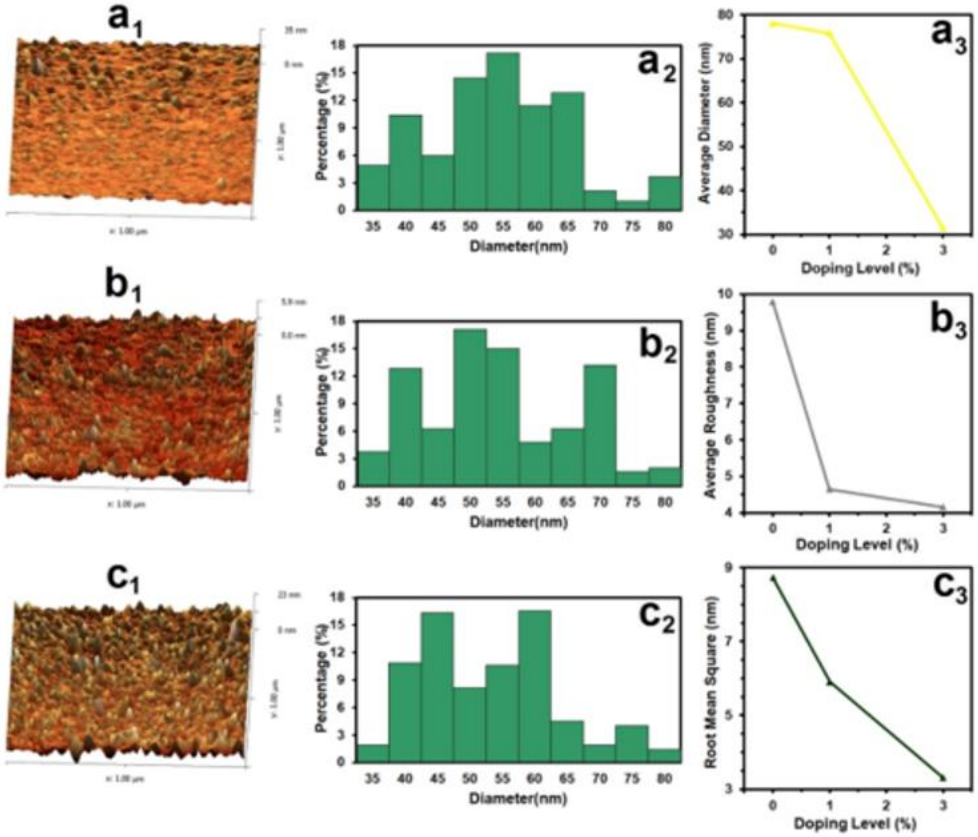

Figure 3: AFM images a_1), b_1), and c_1), granularly distributed a_2), b_2), and c_2) and diversity of AFM parameters against doping a_3), b_3); and c_3).

Refractive index n were calculated by (7) [52]:

$$k = \frac{\alpha\lambda}{4\pi}. \quad (7)$$

The extinction coefficient (k) were determined by (8) [53]:

$$n = \frac{1+R^{\frac{1}{2}}}{1-R^{\frac{1}{2}}}. \quad (8)$$

Figure 7, 8 shows that both n and k values decrease as the wavelength increases. n exhibits a decreasing trend with increasing λ [54], n remain relatively consistent around 450 nm and beyond. The refractive index impacts the optical pathway of light and influences the amount of light reflected from a surface. An increase in n of a solid corresponds to the rise in reflection. Figure 8 depicts k plotted against wavelength for ZnS and Indium-doped ZnS nanocrystals. k reaches their minimum values in the 500-700 nm wavelength range. The decreasing n can be attributed to surface effects and imperfections [55].

The gas sensing properties was done at an operating temperature of 100°C. Figure 9 shows the resistance variation when exhibited to NO_2 gas at a content of 300 ppm. It was observed that ZnS films exhibited the lowest resistance, suggesting a more efficient adsorption of NO_2 molecules [56]. In contrast, the ZnS film doped with 3% Indium demonstrated the highest resistance, likely due to changes in the film's electronic structure and the interaction between the dopant and NO_2 molecules, which might hinder the charge carrier mobility. This indicates that Indium doping increases the resistance and alters the gas sensing properties of the ZnS films [57].

The sensitivity can be calculated using (9) [58]:

$$Sensitivity = \frac{\Delta R}{R_g} = \left|\frac{R_g - R_a}{R_g}\right| \times 100\ \% \quad (9)$$

where R_g represents the resistance of the film sensor in air, and Ra is the resistance in the presence of gas. Figure 10 presents the sensitivity plots illustrating the effects of undoped ZnS, ZnS: 1% In, and ZnS: 3% In on NO_2 gas exposure. The recombination process of

charge carriers between electrons and holes impacts the sensitivity, showing a decrease as the Indium doping concentration increases. Specifically, for undoped, ZnS: 1% In, and ZnS: 3% In, the sensitivity decreases from 42.6% to 8.8 % at 100 ppm, from 48.4 % to 11.3 % at 200 ppm, and from 553.2% to 13.8 % at 300 ppm. This reduction in sensitivity indicates that higher Indium content result in a decline in the sensor's ability to respond to NO_2 gas [59, 60]. This behavior is attributed to the structural changes in the films due to doping process, which affects charge carrier mobility and consequently the sensor's performance [61].

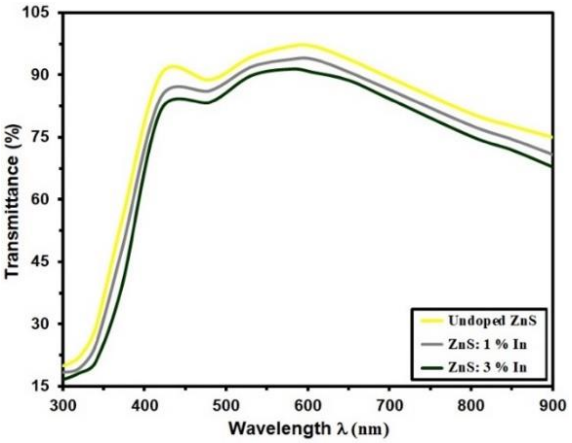

Figure 4: Transmittance of pure and ZnS:In films.

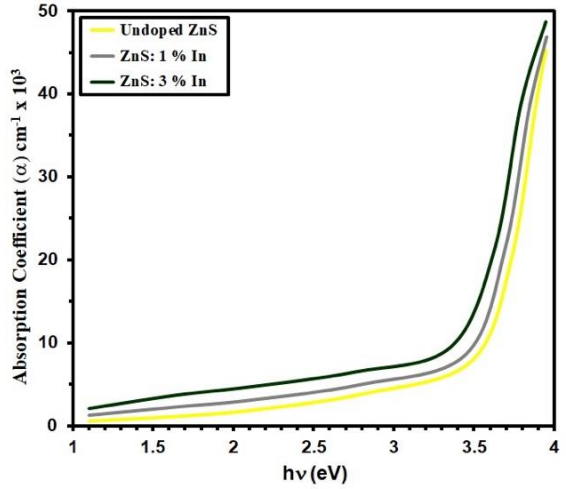

Figure 5: Absorption of pure and ZnS:In films with different dopant.

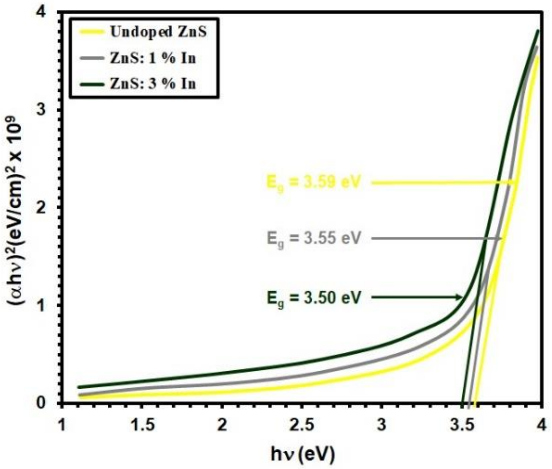

Figure 6: Plot of $(\alpha h\nu)^2$ versus $h\nu$ for pure and ZnS:In films with different dopant levels.

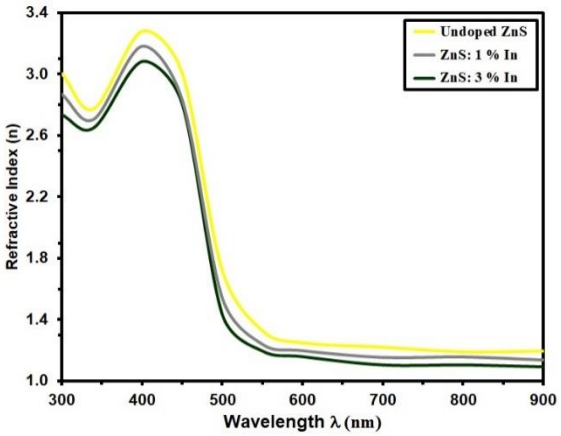

Figure 7: Refractive index (n) of pure and ZnS:In films as a function of wavelength..

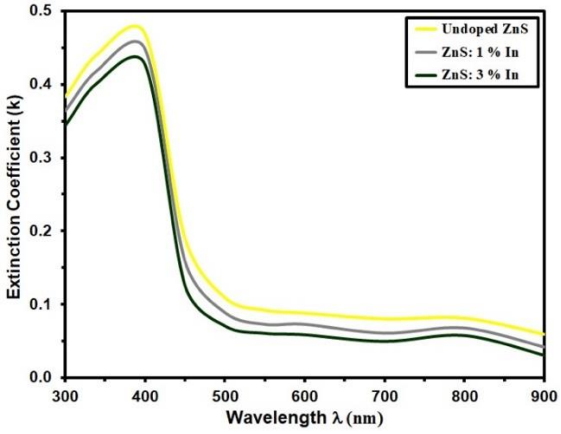

Figure 8: Spectral behavior of the extinction coefficient (k) for ZnS and ZnS:In thin films.

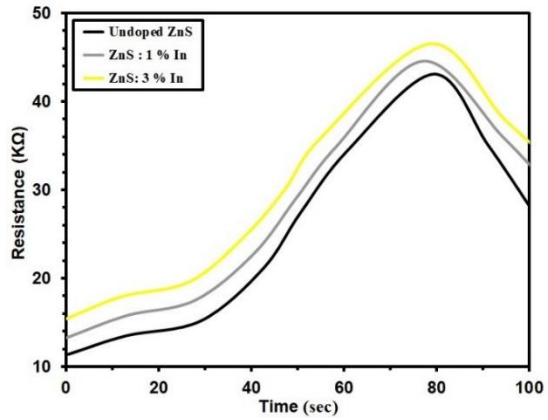

Figure 9: Resistance vs. operating time for undoped ZnS and In-doped ZnS films.

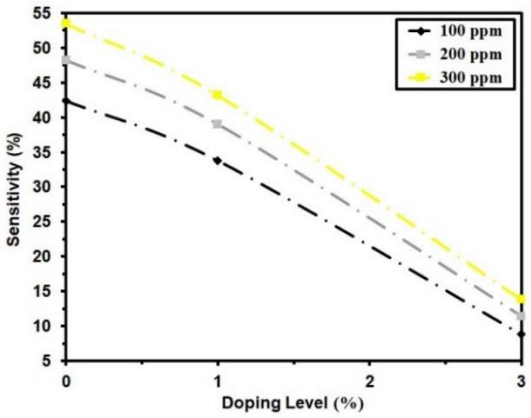

Figure 10: Sensitivity of undoped and ZnS in films with different dopants.

4 CONCLUSIONS

Indium-doped ZnS thin films were deposited using the CSP method. Films containing 0%, 1%, and 3% indium were deposited onto glass substrates at a temperature of 400°C. Structural characterization using X-ray diffraction (XRD) confirmed that all samples maintained a cubic zinc blende structure, with no evidence of secondary phases. As the indium concentration increased, a slight enlargement in crystallite size and a shift in diffraction peaks were observed, indicating successful substitution of Zn^{2+} ions by In^{3+} within the ZnS lattice. These changes also corresponded to a reduction in lattice strain and dislocation density, reflecting enhanced crystal quality. AFM studies reveal changes in film roughness following dopant treatment. The reduction in nano-grain size correlates with the concentration of indium, influenced by the interaction between ZnS and Indium during synthesis. UV-Vis measurements demonstrate a decrease in E_g with increasing Indium content. Additionally, reductions in n and k were observed due to doping, possibly due to the appearance of In3+ ions. Gas sensing tests conducted at 100°C revealed that undoped ZnS films exhibited the highest sensitivity to NO_2 gas. However, increasing the indium doping level led to a marked increase in electrical resistance and a significant decline in gas sensitivity. This reduction in performance is likely caused by decreased charge carrier mobility and increased electron-hole recombination, resulting from the structural and electronic changes induced by doping.

ACKNOWLEDGMENTS

The authors express their gratitude for the support provided by Mustansiriyah University and Alnukhba University College.

REFERENCES

[1] D.H. Hwang, J.H. Ahn, K.N. Hui, K. San Hui, and Y.G. Son, "Structural and optical properties of ZnS thin films deposited by RF magnetron sputtering," Nanoscale Research Letters, vol. 7, pp. 1-7, 2012, [Online]. Available: https://link.springer.com/article/10.1186/1556-276X-7-26 .

[2] S. Ummartyotin and Y. Infahsaeng, "A comprehensive review on ZnS: From synthesis to an approach on solar cell," Renewable and Sustainable Energy Reviews, vol. 55, pp. 17-24, 2016.

[3] J. Kennedy, P. Murmu, P. Gupta, D. Carder, S. Chong, J. Leveneur, and S. Rubanov, "Structural, optical and electrical properties of zinc sulphide thin films synthesized by solution growth technique," Materials Science in Semiconductor Processing, vol. 26, pp. 561-566, 2014.

[4] J. Cheng, D. Fan, H. Wang, B. Liu, Y. Zhang, and H. Yan, "Chemical bath deposition of crystalline ZnS thin films," Semiconductor Science and Technology, vol. 18, no. 7, p. 676, 2003, [Online]. Available: https://doi.org/10.1088/0268-1242/18/7/313 .

[5] N. Kaur, S. Kaur, J. Singh, and M. Rawat, "A review on zinc sulphide nanoparticles: From synthesis, properties to applications," Journal of Bioelectronics and Nanotechnology, vol. 1, no. 1, pp. 1-5, 2016, [Online]. Available: https://doi.org/10.13188/2475-224X.1000006 .

[6] X. Fang, T. Zhai, U.K. Gautam, L. Li, L. Wu, Y. Bando, and D. Golberg, "Modification of the surface properties of core-shell semiconductors and their effects on the photodecolorization activity and adsorption," Progress in Materials Science, vol. 56, pp. 175-287, 2011.

[7] M.E. Pacheco, C.B. Castells, and L. Bruzzone, "Electrical resistance sensor based on ZnO nanoarray for VOC gas detection," Sensors and Actuators B: Chemical, vol. 238, pp. 660-666, 2017.

[8] X. Zhang, D. Wu, X. Zhou, Y. Yu, J. Liu, N. Hu, H. Wang, G. Li, and Y. Wu, "Recent progress in the construction of nanozyme-based biosensors and their applications to food safety assay," TrAC Trends in Analytical Chemistry, vol. 121, p. 115668, 2019.

[9] A. Jrad, T.B. Nasr, and N. Turki-Kamoun, "Optical characteristics of Al-doped ZnS thin film using pulsed laser deposition technique: The effect of aluminum concentration," Journal of Materials Science: Materials in Electronics, vol. 26, no. 11, pp. 8854-8862, 2015.

[10] T. Hurma, "The structural and optical properties of ZnS films obtained by spraying solutions at different molarities," Materials Today: Proceedings, 2019, [Online]. Available: https://doi.org/10.1016/j.matpr.2019.06.676 .

[11] M.B.A. Bashir, M.F.M. Sabri, S.M. Said, Y. Miyazaki, I.A. Badruddin, D.A.A. Shnawah, E.Y. Salih, S. Abushousha, and M.H. Elsheikh, "Enhancement of thermoelectric properties of Co4Sb12 skutterudite by Al and La double filling," Journal of Solid State Chemistry, vol. 284, p. 121205, 2020.

[12] H. Benamra, H. Saidi, A. Attaf, M. Aida, A. Derbali, and N. Attaf, "Physical properties of Al-doped ZnS thin films prepared by ultrasonic spray technique," Surfaces and Interfaces, vol. 21, p. 100645, 2020, [Online]. Available: https://doi.org/10.1016/j.surfin.2020.100645 .

[13] A. Azmand and H. Kafashan, "Al-doped ZnS thin films: Physical and electrochemical characterizations," Journal of Alloys and Compounds, 2019, [Online]. Available: https://doi.org/10.1016/J.JALLCOM.2018.11.268 .

[14] A. Dhupar, S. Kumar, H.S. Tuli, A.K. Sharma, V. Sharma, and J. Kumar, "In-doped ZnS nanoparticles: Structural, morphological, optical and antibacterial properties," Applied Physics A, vol. 127, no. 4, p. 263, 2021.

[15] A.S. Baranski, M.S. Bennet, and W.R. Fawcett, "The physical properties of CdS thin films electrodeposited from aqueous diethylene glycol solutions," Journal of Applied Physics, vol. 54, no. 11, pp. 6390-6394, 1983.

[16] A.U. Ubale and D.K. Kulkarni, "Preparation and study of thickness-dependent electrical characteristics of zinc sulfide thin films," Bulletin of Materials Science, vol. 28, no. 1, pp. 43-47, 2005.

[17] A. Goudarzi, G.M. Aval, R. Sahraei, and H. Ahmadpoor, "Ammonia-free chemical bath deposition of nanocrystalline ZnS thin film buffer layer for solar cells," Thin Solid Films, vol. 516, no. 15, pp. 4953-4957, 2008.

[18] T.M. Thi, N.T. Hien, D.X. Thu, and V.Q. Trung, "Thin films containing Mn-doped ZnS nanocrystals synthesised by chemical method and study of some of their optical properties," Journal of Experimental Nanoscience, vol. 8, no. 5, pp. 694-702, 2012.

[19] E. Turan, M. Zor, A.S. Aybek, and M. Kul, "Electrical properties of ZnO/Au/ZnS/Au films deposited by ultrasonic spray pyrolysis," Thin Solid Films, vol. 515, no. 24, pp. 8752-8755, 2007.

[20] W. Daranfed, M.S. Aida, A. Hafdallah, and H. Lekiket, "Substrate temperature influence on ZnS thin films prepared by ultrasonic spray," Thin Solid Films, vol. 518, no. 4, pp. 1082-1084, 2009.

[21] I. Yu, T. Isobe, and M. Senna, "Optical properties and characteristics of ZnS nano-particles with homogeneous Mn distribution," Journal of Physics and Chemistry of Solids, vol. 57, no. 4, pp. 373-379, 1996, [Online]. Available: https://doi.org/10.1016/0022-3697(95)00285-5 .

[22] H.T. Salloom, E.H. Hadi, N.F. Habubi, S.S. Chiad, M. Jadan, and J.S. Addasi, "Characterization of silver content upon properties of nanostructured nickel oxide thin films," Digest Journal of Nanomaterials and Biostructures, vol. 15, no. 4, pp. 1189-1195, 2020.

[23] C.K. De and N.K. Mishra, "Synthesis and characterisation of co-evaporated tin sulphide thin films," Indian Journal of Physics A, vol. 71, no. 5, p. 530, 1997.

[24] R.S. Ali, N.A.H. Al Aaraji, E.H. Hadi, K.H. Abass, N.F. Habubi, and S.S. Chiad, "Effect of lithium on structural and optical properties of nanostructured CuS thin films," Journal of Nanostructures, vol. 10, no. 4, pp. 810-816, 2020.

[25] M. Bedir, A. Tunç, and M. Oztas, "Investigation of the characteristics of the boron doped MnO films deposited by spray pyrolysis method," Acta Physica Polonica A, vol. 129, no. 6, pp. 1091-1093, 2016.

[26] K. Murakami, K. Nakajima, and S. Kaneko, "Initial growth of SnO2 thin film on the glass substrate deposited by the spray pyrolysis technique," Thin Solid Films, vol. 515, no. 24, pp. 8632-8636, 2007, [Online]. Available: https://doi.org/10.1016/J.TSF.2007.03.128 .

[27] T. Jiang, N. Hall, A. Ho, and S. Morin, "Quantitative analysis of electrodeposited tin film morphologies by atomic force microscopy," Thin Solid Films, vol. 471, pp. 76-85, 2005, [Online]. Available: https://doi.org/10.1016/J.TSF.2004.04.051 .

[28] K. Santhosh Kumar, C. Manoharan, S. Dhanapandian, and A. Gowri Manohari, "Effect of Sb dopant on the structural, optical and electrical properties of SnS thin films by spray pyrolysis technique," Spectrochimica Acta Part A: Molecular and Biomolecular Spectroscopy, vol. 115, pp. 840-844, 2013.

[29] A. Azmand and H. Kafashan, "Al-doped ZnS thin films: Physical and electrochemical characterizations," Journal of Alloys and Compounds, 2019, [Online]. Available: https://doi.org/10.1016/J.JALLCOM.2018.11.268 .

[30] R.M. Ibrahim, M. Markom, and K.F. Abd Razak, "Optical properties of Fe^{2+} ion doped ZnS nanoparticles synthesized using co-precipitation method," Jurnal Kejuruteraan, vol. 27, pp. 87-94, 2015.

[31] A.A. Khadayeir, R.I. Jasim, S.H. Jumaah, N.F. Habubi, and S.S. Chiad, "Influence of substrate temperature on physical properties of nanostructured ZnS thin films," Journal of Physics: Conference Series, vol. 1664, no. 1, p. 012055, 2020.

[32] S. Sapra, J. Nanda, A. Anand, S.V. Bhat, and D.D. Sarma, "Optical and magnetic properties of manganese-doped zinc sulfide nanoclusters," Journal of Nanoscience and Nanotechnology, vol. 3, no. 5, pp. 392-400, 2003, [Online]. Available: https://doi.org/10.1166/JNN.2003.211 .

[33] S.S. Chiad, A.S. Alkelaby, and K.S. Sharba, "Optical conduct of nanostructure Co_3O_4-rich highly doped Co_3O_4:Zn alloys," Journal of Global Pharma Technology, vol. 11, no. 7, pp. 662-665, 2020.

[34] F. Aghaei, R. Sahraei, E. Soheyli, and A. Daneshfar, "Dopant-concentration dependent optical and structural properties of Cu-doped ZnS thin films," Journal of Nanostructures, vol. 12, no. 2, pp. 330-342, 2022.

[35] B.Y. Geng, X.W. Liu, Q.B. Du, X.W. Wei, and L.D. Zhang, "Structural, morphological and optical properties of Mn doped ZnS nanocrystals," Applied Physics Letters, vol. 88, no. 16, p. 163104, 2006.

[36] S.S. Chiad, H.A. Noor, O.M. Abdulmunem, and N.F. Habubi, "Optical and structural properties of Ni-doped Co_3O_4 nanostructure thin films via CSPM," Journal of Physics: Conference Series, vol. 1362, no. 1, p. 012125, 2019.

[37] A. Jrad, T. Ben Nasr, and N. Turki-Kamoun, "Study of structural, optical and photoluminescence properties of indium-doped zinc sulfide thin films for optoelectronic applications," Optical Materials, vol. 50, pp. 128-133, 2015.

[38] R.S. Ali, M.K. Mohammed, A.A. Khadayeir, Z.M. Abood, N.F. Habubi, and S.S. Chiad, "Structural and optical characterization of sprayed nanostructured indium doped Fe_2O_3 thin films," Journal of Physics: Conference Series, vol. 1664, no. 1, p. 012016, 2020.

[39] A. El Hichou, M. Addou, J.L. Bubendorff, J. Ebothé, B. El Idrissi, and M. Troyon, "Microstructure and cathodoluminescence study of sprayed Al and Sn doped ZnS thin films," Semiconductor Science and Technology, vol. 19, no. 2, pp. 230-236, 2003.

[40] G. Gordillo and E. Romero, "Structural characterization of thin films based on II–VI ternary compounds deposited by evaporation," Thin Solid Films, vol. 484, no. 1-2, pp. 352-357, 2005.

[41] M. Ashraf, S.M.J. Akhtar, M. Mehmood, and A. Qayyum, "Optical and structural properties of ZnS_xSe_{1-x} thin films deposited by thermal evaporation," European Physical Journal - Applied Physics, vol. 48, no. 4, p. 40101, 2009.

[42] X. Fang, T. Zhai, U.K. Gautam, L. Li, L. Wu, Y. Bando, and D. Golberg, "ZnS nanostructures: From synthesis to applications," Progress in Materials Science, vol. 56, no. 2, pp. 175-287, 2011.

[43] S. Xue, "Effects of thermal annealing on the optical properties of Ar ion irradiated ZnS films," Ceramics International, vol. 39, no. 6, pp. 6577-6581, 2013.

[44] C. Jin, H. Kim, K. Baek, and C. Lee, "Effects of coating and thermal annealing on the photoluminescence properties of ZnS/ZnO one-dimensional radial heterostructures," Materials Science and Engineering B, vol. 170, no. 1-3, pp. 143-148, 2010.

[45] Z. Zhang, D. Shen, J. Zhang, C. Shan, Y. Lu, Y. Liu, B. Li, D. Zhao, B. Yao, and X. Fan, "The growth of single cubic phase ZnS thin films on silica glass by plasma-assisted metalorganic chemical vapor deposition," Thin Solid Films, vol. 513, no. 1-2, pp. 114-117, 2006.

[46] P. Luque, A. Castro-Beltrán, A. Vilchis-Nestor, M. Quevedo-López, and A. Olivas, "Influence of pH on properties of ZnS thin films deposited on SiO_2 substrate by chemical bath deposition," Materials Letters, vol. 140, pp. 148-150, 2015.

[47] B. Elidrissi, M. Addou, M. Regragui, A. Bougrine, A. Kachouane, and J. Bernède, "Structure, composition and optical properties of ZnS thin films prepared by spray pyrolysis," Materials Chemistry and Physics, vol. 68, no. 1-3, pp. 175-179, 2001.

[48] K. Wright, G.W. Watson, and S.C. Parker, "Simulation of the structure and stability of sphalerite (ZnS) surfaces," American Mineralogist, vol. 83, no. 1-2, pp. 141-146, 1998.

[49] B.D. Cullity, Elements of X-ray Diffraction, 2nd ed. Boston, MA, USA: Addison-Wesley, 1978.

[50] A.K. Kole and P. Kumbhakar, "Cubic-to-hexagonal phase transition and optical properties of chemically synthesized ZnS nanocrystals," Results in Physics, vol. 2, pp. 150-155, 2012.

[51] M. Ashraf, M. Mehmood, and A. Qayyum, "Influence of source-to-substrate distance on the properties of ZnS films grown by close-space sublimation," Semiconductors, vol. 46, no. 10, pp. 1326-1330, 2012.

[52] K. Benyahia, A. Benhaya, and M.S. Aida, "ZnS thin films deposition by thermal evaporation for photovoltaic applications," Journal of Semiconductors, vol. 36, no. 10, p. 103001, 2015.

[53] F. Özütok, K. Ertürk, and V. Bilgin, "Growth, electrical, and optical study of ZnS:Mn thin films," Acta Physica Polonica A, vol. 121, no. 1, pp. 128-132, 2012.

[54] A. Derbali, A. Attaf, H. Saidi, M. Aida, H. Benamra, R. Attaf, N. Attaf, and H. Ezzaouia, "Br doping effect on structural, optical and electrical properties of ZnS thin films deposited by ultrasonic spray," Materials Science and Engineering B, vol. 268, p. 115135, 2021.

[55] P. Chelvanathan, Y. Yusoff, F. Haque, M. Akhtaruzzaman, M. Alam, Z. Alothman, M. Rashid, K. Sopian, and N. Amin, "Growth and characterization of RF-sputtered ZnS thin film deposited at various substrate temperatures for photovoltaic application," Applied Surface Science, vol. 334, pp. 138-144, 2015.

[56] R. Zhang, B. Wang, and L. Wei, "Influence of RF power on the structure of ZnS thin films grown by sulfurizing RF sputter-deposited ZnO," Materials Chemistry and Physics, vol. 112, no. 2, pp. 557-561, 2008.

[57] T.S. Moss, Optical Properties of Solids. London, U.K.: Butterworths, 1961.

[58] M. Caglar, Y. Caglar, and S. Ilican, "Investigation of the effect of Mg doping for improvements of optical and electrical properties," Physica B: Condensed Matter, vol. 485, pp. 6-10, 2016.

[59] T. Mahalingam, V. Dhanasekaran, G. Ravi, S. Lee, J.P. Chu, and H.J. Lim, "Effect of deposition potential on the physical properties of electrodeposited CuO thin films," Journal of Optoelectronics and Advanced Materials, vol. 12, no. 6, pp. 1327-1332, 2010.

[60] S. Sen, S.K. Halder, and S.P. Sen Gupta, "An x-ray line shift analysis in vacuum-evaporated silver films," Journal of the Physical Society of Japan, vol. 38, no. 6, pp. 1643-1649, 1975.

[61] P. Bhuvaneswari and M. Velusamy, "Effect of fluorine doping on the structural, optical and electrical properties of spray deposited cadmium stannate thin films," Materials Science in Semiconductor Processing, vol. 16, no. 6, pp. 1964-1970, 2013.